Biochimica et Biophysica Acta 1827 (2013) 949–957

Contents lists available at SciVerse ScienceDirect

Biochimica et Biophysica Acta

journal homepage: www.elsevier.com/locate/bbabio

Review

Designing interfaces of hydrogenase–nanomaterial hybrids for efficient solar conversion ☆

Paul W. King *

National Renewable Energy Laboratory, Biosciences Center, Golden, CO 80401, USA

ARTICLE INFO

Article history:
Received 28 January 2013
Accepted 18 March 2013
Available online 27 March 2013

Keywords:
Interface
Electron-transfer
Nanoparticle
Photocatalysis
Enzyme biohybrid
Solar conversion

ABSTRACT

The direct conversion of sunlight into biofuels is an intriguing alternative to a continued reliance on fossil fuels. Natural photosynthesis has long been investigated both as a potential solution, and as a model for utilizing solar energy to drive a water-to-fuel cycle. The molecules and organizational structure provide a template to inspire the design of efficient molecular systems for photocatalysis. A clear design strategy is the coordination of molecular interactions that match kinetic rates and energetic levels to control the direction and flow of energy from light harvesting to catalysis. Energy transduction and electron-transfer reactions occur through interfaces formed between complexes of donor–acceptor molecules. Although the structures of several of the key biological complexes have been solved, detailed descriptions of many electron-transfer complexes are lacking, which presents a challenge to designing and engineering biomolecular systems for solar conversion. Alternatively, it is possible to couple the catalytic power of biological enzymes to light harvesting by semiconductor nanomaterials. In these molecules, surface chemistry and structure can be designed using ligands. The passivation effect of the ligand can also dramatically affect the photophysical properties of the semiconductor, and energetics of external charge-transfer. The length, degree of bond saturation (aromaticity), and solvent exposed functional groups of ligands can be manipulated to further tune the interface to control molecular assembly, and complex stability in photocatalytic hybrids. The results of this research show how ligand selection is critical to designing molecular interfaces that promote efficient self-assembly, charge-transfer and photocatalysis. This article is part of a Special Issue entitled: Metals in Bioenergetics and Biomimetics Systems.

1. Introduction

Electron-transfer reactions constitute a fundamental process of energy transduction in biology that link biochemical reactions to the metabolic pathways that are essential for cellular life. These pathways function to convert abundant substrates such as solar energy, water, carbon dioxide, nitrogen and oxygen into the energy carrying molecules necessary for cellular viability [1]. A majority of the conversion steps are redox-driven, where photoelectrochemical potential derived from light-harvesting by photosynthetic reaction centers provides the energy and driving force for downstream enzymatic formation of hydrogen (H_2) and other biofuel compounds [2,3]. These enzymatic steps are coupled to electron-transfer (ET), which is mediated by the diffusion controlled formation of transient protein–protein complexes. The resulting binding surface, or interface, functions as part of the medium through which electrons are transferred. Thus, a co-evolution of protein structures and binding surfaces, cofactor redox potentials and solvent networks contribute to geometric and thermodynamic parameters that control ET rates [4]. Understanding the complexity of the molecular interactions that control electron flow presents one of many challenges to reengineering photosynthetic solar-energy conversion for the large-scale production of energy carriers [5–7].

The functional themes that control biological photoconversion are also fundamental to the development of efficient charge-transfer and catalysis in artificial photosynthetic systems. Interest in developing chemical based approaches to solar fuel production has gained significant momentum in recent years and many strategies are being developed that include mixing synthetic and biological components [8–18]. One approach to motivate and inspire artificial efforts has been to use

Abbreviations: AA, ascorbic acid; BET, back electron-transfer; CB, conduction band; CdS, cadmium sulfide; CdTe, cadmium telluride; CS, charge-separation; CT, charge-transfer; CytC, Cytochrome *C*; DFT, density functional theory; DHA, dehydroascorbate; EC-STM, electrochemical scanning tunneling microscopy; E_g, band gap energy; ET, electron-transfer; eV, electron volt; FB, flat-band; HT, hole-transfer; MPA, mercaptopropionic acid; MWNT, multi-walled carbon nanotubes; NP, nanoparticle; PC, plastocyanin; PSI, Photosystem I; QY, quantum yield; RuP, ruthenium bipyridine phosphonic acid; SAM, self-assembled monolayer; ST, surface–trap; SWNT, single-walled carbon nanotubes; TEOA, triethanolamine; TiO_2, titanium dioxide; VB, valence band; VDW, van der Waal

☆ This article is part of a Special Issue entitled: Metals in Bioenergetics and Biomimetics Systems.

* Tel.: +1 303 384 6277; fax: +1 303 384 3847.
E-mail address: paul.king@nrel.gov.

0005-2728/$ – see front matter © 2013 Elsevier B.V. All rights reserved.
http://dx.doi.org/10.1016/j.bbabio.2013.03.006

enzymes as catalysts in solar conversion devices and photocatalytic complexes [19–26]. The substrate specificities, high turnover rates, low reaction overpotentials and the use of base transition metals (e.g., Fe, Ni, Cu, and Mg) make enzymes an attractive option for use in photocatalytic systems [24]. Significant progress has been made toward interfacing enzymes with organic and inorganic materials for photochemical conversion. Examples include direct immobilization of enzymes on electrodes (e.g., bulk and nanostructured carbon [27–32], TiO_2 [33–35], Au [30,36,37]), and in molecular complexes with photoactive and conductive materials (e.g., macroscopic [38–40] and nanoparticulate inorganic semiconductors [41–45], carbon-based particles and nanorods [46,47]) (Fig. 1). The combination of high catalytic rates exhibited by enzymes and the outstanding photophysical properties and high molar extinction coefficients of nanomaterials has the potential to exceed photosynthetic light-harvesting efficiencies when electronically coupled to enzymes [5,23,48]. Moreover, the demonstration of multi-exciton generation, or a >1 ratio of electron-hole pairs per absorbed photon in nanoparticle (NP) based photovoltaics, is driving even greater interest in these materials for use as light harvesting molecules in the production of solar fuels [49,50].

The success of these efforts and the potential for high conversion efficiencies have led to more effort to understand the factors that control the fundamental processes of molecular assembly, ET and photocatalysis. As in biological ET, the interface in enzyme-semiconductor complexes has an essential role in each of these processes. Interfaces mediate molecular assembly and the spatial relationship of molecules, alter the energy landscape through surface passivation and mediate charge-transfer reactions, all of which control photocatalytic performance. This review will present a brief summary of basic ET theory for context, discuss how NP interfaces control solar conversion energetics, and highlight examples of enzyme-NP photocatalytic hybrids that include complexes of [FeFe]-hydrogenases and semiconducting NPs for solar-driven H_2 production.

2. Biological electron-transfer

A general model for ET mechanisms in proteins and protein complexes has emerged from extensive experimental and theoretical efforts, and generally conforms to the basic principles of nonadiabatic ET

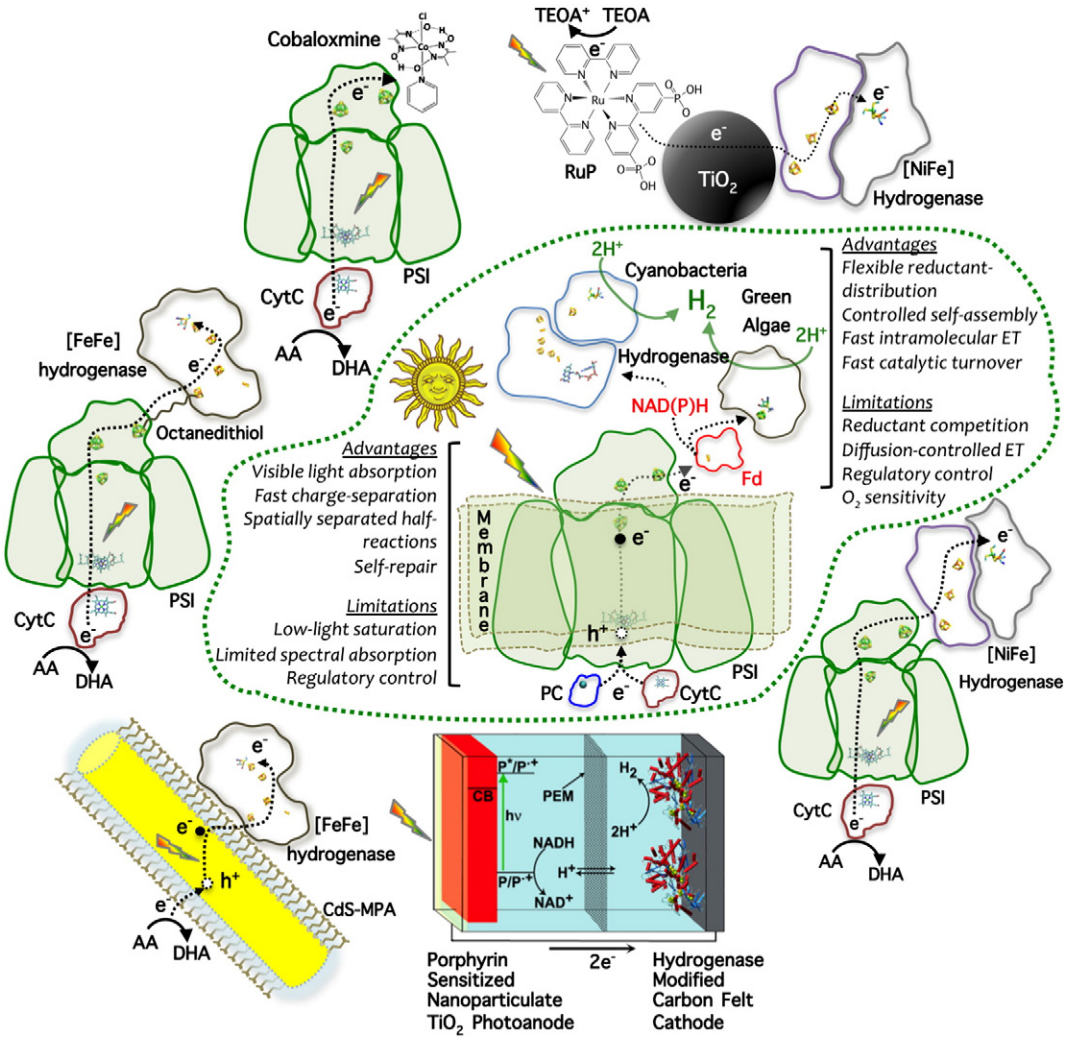

Fig. 1. Bio-inspired, enzyme-based hybrid complexes and devices directly couple the catalytic power of enzymes and catalysts with light-harvesting by natural photosystems (PSI), artificial NPs, or photoelectrochemical cells for solar H_2 production. The center panel shows the biomolecules that together function to direct solar energy capture and conversion by cyanobacterial or algal photosynthesis to enzymatic H_2 production by hydrogenases. Some of the advantages and limitations of photobiological H_2 production systems are identified. Examples of biomolecular, bio-inspired and enzyme-NP hybrid systems are shown clockwise from the left: PSI-CytC chemically linked to a [FeFe]-hydrogenase by octanedithiol [51]; cobaloxmine adsorbed to PSI [52]; [NiFeSe]-hydrogenase adsorbed to particulate, dye-sensitized TiO_2 [45]; [NiFe]-hydrogenase genetically fused to the *psaE* subunit of PSI [53–55]; [FeFe]-hydrogenase adsorbed onto a carbon electrode in a dye-sensitized photoelectrochemical cell (adapted with permission from ACS, [29]); and [FeFe]-hydrogenase adsorbed to MPA passivated CdS nanorods [42].

as described by Marcus Theory (Eq. (1)) [56]. The influence of the interfacial dielectric and solvation properties, donor–acceptor edge-to-edge distances and orientations (β), donor–acceptor energy levels (ΔG), electronic wavefunction overlap ($|H_{AB}|$), and nuclear reorganization energy (λ) together comprise the parameters that control overall ET transfer rates. The physical manifestations of these parameters in terms of the structural and energetic properties of the proteins and photosynthetic reaction centers have been explored [5,7,48,57,58], and basic mechanistic principles have been developed [59–61].

$$k_{ET} = \frac{2\pi}{\hbar}|H_{AB}|^2 \frac{1}{\sqrt{4\pi\lambda k_b T}} e\left(-\frac{(\lambda + \Delta G^\circ)^2}{4\lambda k_b T}\right) \quad (1)$$

To examine the effect of changing donor–acceptor edge-to-edge distance (d) on a molecular system with a reaction rate k (k_{ET} for direct measurement of ET), Eq. (1) can be simplified to show the exponential relationship of k_{ET} to distance, d, including the effects of the intervening medium, β, as shown in Eq. (2) [62] for in a number of experimental systems. Values of β have been experimentally determined for transfer through conjugated alkane (0.8–1.2 $Å^{-1}$) or xylyl (0.4–0.8 $Å^{-1}$) ligands, and for long-range intramolecular ET through proteins (~1.1 $Å^{-1}$) [59,60,63].

$$k = k_0 e^{-\beta d} \quad (2)$$

In the context of enzyme-NP hybrids and other photocatalytic complexes and devices, the interfacial composition of the semiconducting surface can influence the ET process through effects on β (distance effect on electronic coupling), $|H_{AB}|$ (angular and distance effects on orbital–orbital interactions) and λ (effect of solvation and dielectric). Extrapolation of biological design principles to the development of optimal ET in hybrids also includes the interfacial medium that is formed upon by adsorption of an enzyme to the material, for example an electrode or NP surface. If this surface interaction creates a complex that is sufficiently desolvated, with favorable electrostatic contacts and sufficiently large contact surface area, a stable CT complex can be created to support a direct energy conversion process that is not subject diffusion controlled ET.

3. Photosynthetic hydrogen production, protein–protein complexes and terminal ET reaction steps

To achieve an overall forward process of directing energy flow from reaction centers to terminal electron acceptors and ultimately to the enzymes that catalyze fuel production, photosystems structurally evolved to minimize the probability of back electron transfer (BET) [7,58,64,65]. For example, through engineering the Δ*G or* λ parameter of a particular transfer step, the BET reaction can be several orders of magnitude slower than forward ET, without inhibiting the overall forward flow of the process. Protein–protein complexes involved in ET are largely controlled by complementary electrostatic interactions [66], with interfaces involving van der Waals (VDW) contacts between charged and non-polar residues [67]. Also included as determining factors are shape complementarity, and hydrophobic interactions that create a surface contact area, which for biological complexes is typically in the range of ~1200 $Å^2$ [67].

In the case of biological H_2 production by [FeFe]-hydrogenases, the ET step can be facilitated by different types of electron carrier proteins [68–70] including ferredoxins, small molecular weight proteins that harbor metallo-centers in the form of [2Fe–2S] (algae and higher plants) or [4Fe–4S] (bacteria) clusters. The surfaces adjacent to FeS clusters in ferredoxins are typically rich in acidic residues, which contribute in facilitating electrostatic interactions with the positive surfaces on [FeFe]-hydrogenases (Fig. 2). These positive surfaces surround distal FeS clusters of [FeFe]-hydrogenase, which vary in both cluster type and quantity among different enzyme sub-groups [71–73]. In addition, non-polar residues are often located within the electrostatic contact surface (Fig. 2, right), and the resulting hydrophobic interactions are predicted to have a role in controlling close-packing and solvation of the ET interface [74]. In green algae, the terminal ET step in light-driven H_2 production involves formation of a protein–protein complex between [2Fe–2S] ferredoxin and [FeFe]-hydrogenase [63,75]. Models of this complex have proposed that the ET interface consists of surface of ~900 $Å^2$ with electrostatic and hydrophobic contacts between conserved polar and non-polar residues both on the ferredoxin and on the hydrogenase [76–78]. One objective for the design of [FeFe]-hydrogenase-NP hybrid complexes capable of solar-driven H_2 production has been to mimic the electrostatic interactions that guide formation of natural ET complexes, which is discussed in more detail below. Binding constants for complexes between [FeFe]-hydrogenase and negatively charged, mercaptopropionic acid (MPA) capped CdS and CdTe NPs were measured and showed values ~34-fold higher than for ferredoxin [41,79].

The X-ray structure of [FeFe]-hydrogenase CpI from *Clostridium pasteurianum* (Fig. 2, bottom) revealed a series of accessory FeS clusters that form a ET network connecting surface localized [4Fe–4S] and [2Fe–2S] clusters to the catalytic site H-cluster [81,82]. Based on the distance calculations shown in Fig. 2, an overall ΔG_{pH7} of −0.02 V (based on E_m measurements from titration of electron paramagnetic resonance signals [83]), and using an assumed value for λ of 0.7 eV, the intramolecular ET rate in CpI can be estimated to occur in the range of 10^7–10^{10} s^{-1} [60]. Protein film voltammetry [84,85] and electrochemical scanning tunneling microscopy (EC-STM) techniques have been used to measure catalytic turnover rates of enzymes where interfacial ET is not subject to diffusional control. For CaI, a close homologue of CpI, EC-STM of enzymes immobilized onto carboxy-terminated self-assembled monolayers (SAMs) of alkane thiols on Au electrodes showed a k_{CAT} value of ~10^4 s^{-1} at an overpotential of 0.15 V [86]. Exchange current densities have not been measured for [FeFe]-hydrogenases, and the k_{CAT} value may exceed this value. Nevertheless, the predicted intramolecular ET rate for CpI identifies a threshold upper limit for the design and engineering of interfacial ET in hybrids and other artificial systems that utilize this enzyme.

4. Interfaces and control of molecular assembly, electron-transfer and photocatalysis

Devices for solar H_2 production based on both tandem cells (e.g., Grätzel cell) and solution-phase photocatalytic donor–acceptor complexes have been developed for utilization with enzymes. In each type of design, the electrons must transfer across the material-enzyme interface to drive catalysis. Interfacial properties are determined by the chemical composition of the material surface, which can be modified by chemical functionalization, or by passivation with small molecular weight ligands (Fig. 3). In the case of semiconducting NPs, termination or surface capping with small molecular weight ligands functions to; (i) increase solubility in aqueous buffers [87], (ii) passivate surface defects that otherwise act as non-productive traps for charge recombination, and (iii) stabilize the crystal lattice and control the particle size regime and band-edge energies [88–90]. The first effect is fundamentally important in the self-assembly process and maintaining complex stability over the period of photocatalysis. The second effect plays an important role in determining how photoexcited electrons are partitioned among various relaxation pathways (Fig. 4). The third effect contributes to determining the overall energetics of the hybrid system. Due to the quantum confinement effect the optical valence band (VB) and conduction band (CB) energies vary inversely with NP diameter [91]. These determine flat-band (FB) or oxidation/reduction potentials of NP surface states, and thus the ΔG available to drive the surface localized redox reactions (Fig. 5A). In addition, the band-gap energy (E_g) required for photoexcitation also scales inversely with diameter,

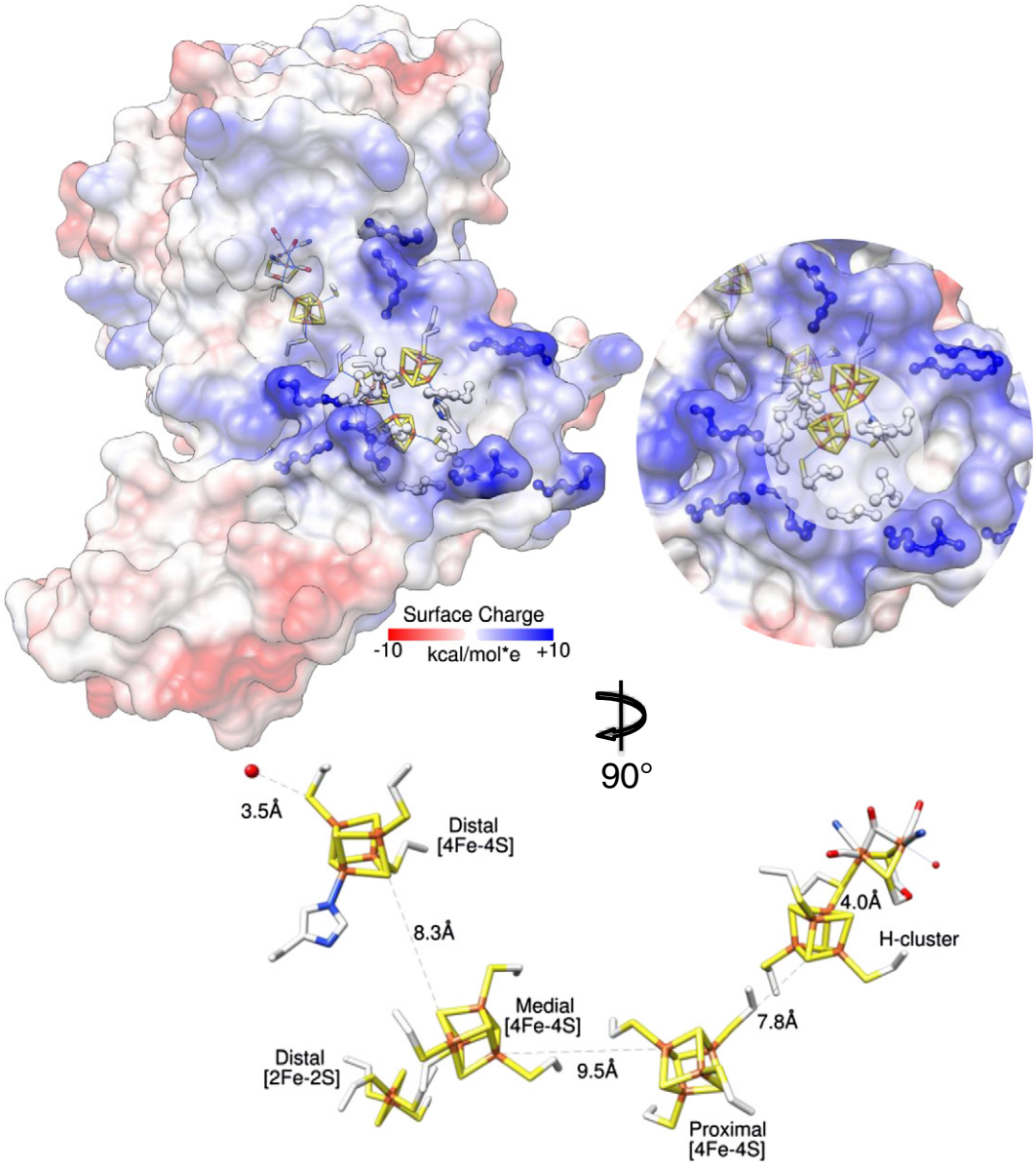

Fig. 2. Electrostatic map and FeS cluster donor–acceptor distances in *Clostridial* [FeFe]-hydrogenase. Top left, the X-ray structure of *Clostridium pasteurianum* [FeFe]-hydrogenase CpI (PDB ID: 3C8Y [80]) rendered with a transparent electrostatic surface (blue = positive, red = negative, white = neutral). The accessory and catalytic FeS clusters are shown with the distal [4Fe–4S] nearest in view. Top right, a close-up view of the surface surrounding the distal [4Fe–4S] cluster showing a ring of basic residues (blue ball and stick) that form a positive electrostatic surface and predicted to make VDW contacts with acidic residues on ferredoxin in an ET complex. Hydrophobic residues (white ball and stick) that contribute to a non-polar surface (white) are located immediately adjacent to the distal [4Fe–4S] cluster. Bottom, the FeS clusters of the CpI structure showing the edge-to-edge distances between each adjacent cluster. A red probe is shown to identify the distance of the protein–solvent interface.

and is largely determined by the bulk material composition of the NP (Fig. 5B) [92].

4.1. Role of the interface in controlling nanoparticle photophysics and interfaces for electron-transfer

Ligand termination or capping of semiconducting NPs, or the non-covalent surface adsorption of ligands onto carbon-based NPs, can significantly alter the configurations of NP surface states. The covalent or π-stacking interactions affect NP surface dielectric, solvation, and bonding properties with significant contributions to the overall NP photophysical properties. Yang et al. have studied the effects of ligand passivation on the band-edge energy levels of semiconducting NPs using density functional theory (DFT) and many-body perturbation theory [99]. Due to (i) surface dipole effects of ligand-NP binding and (ii) the intrinsic dipole of the ligand, the band-edge potentials of passivated versus unpassivated NPs shift in energy relative to photocatalytic (e.g., water splitting) redox reactions (Fig. 5b). The effect of (i) which is manifested as the surface interaction between the ligand and NP, differs depending on the chemical functionality (N or S) of the binding group, whereas the effect of (ii) was sensitive to ligand bond saturation and solvent group functionalization. Together these effects were calculated to induce a >1 eV shift in tunability of the E_{VB}/E_{CB} alignments.

In addition to the effects of ligand binding on controlling surface dielectric properties, thiol passivation has also been shown to enhance photoconversion efficiencies of NP based photovoltaic devices through passivation of traps, thereby increasing radiative lifetimes and exciton dissociation yields for subsequent collection of free carriers [100]. These effects manifest as increased rates of radiative recombination (k_{RR}) detected as an increase in photoluminescence (PL) of NPs (Fig. 4). An increase in the PL efficiency of NPs (η_{PL}, Eq. (3)) has been shown to directly correlate to higher ET and photocatalytic H_2 production

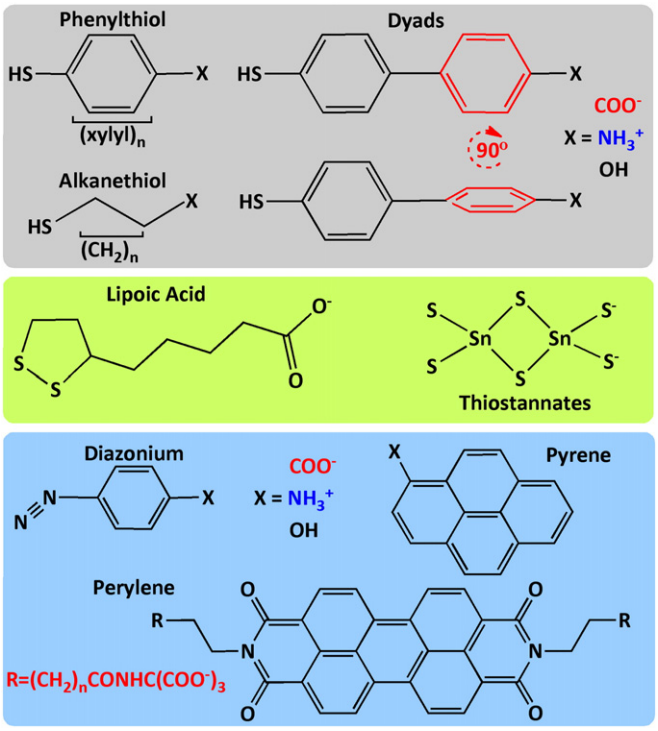

Fig. 3. Ligand structures. Gray panel: Left, aromatic (xylyl) or alkane linkers with S-termination bind the semiconductor surface, leaving the exposed functional groups for enzyme adsorption. Right, molecular dyads with rotation of the biphenyl linker (shown in red) through substitutions at the 2,2′ positions. Rotation changes the relative orientations of orbitals and can be used to control interfacial CT kinetics [93]. Green panel: Bidentate thiol-terminated linkers, lipoic acid [94] and thiostannates [95], with exposed negatively charged carboxyl or sulfhydryl groups. Blue panel: Covalent crosslinking via the azide group of diazonium has been used for attachment to Au or carbon NPs [96]. The π–π stacking between planar aromatic ligands (e.g., pyrene and perylene) [97,98] on hydrophobic surfaces creates a charge-transfer network, with exposed functional groups that can be selectively modified to control enzyme or catalyst attachment and orientation.

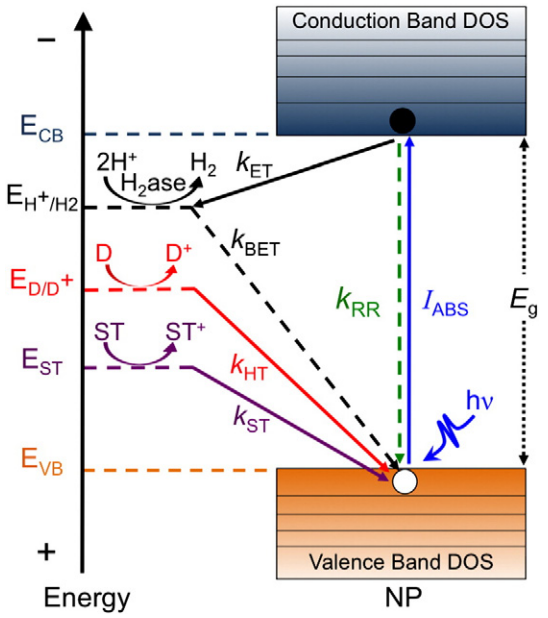

Fig. 4. Energy diagram of the relaxation pathways in photoexcited [FeFe]-hydrogenase NP hybrids. Absorption ($I_{ABS} \propto$ solar flux) of a photon ($h\nu$) with an energy $E \geq E_g$ by a NP results in a charge-separated state and creation of an electron-hole pair. Internal recombination via radiative decay (k_{RR}) results in photoluminescence. Alternatively, the CB electrons can undergo external transfer (k_{ET}) to surface redox couples, for example, hydrogenases (H_2ase), for catalytic H_2 production. Charge balance and regeneration of the NP ground state can be maintained by diffusion mediated hole-scavenging (k_{HT}) using a soluble donor molecule (e.g., ascorbic acid and TEOA) provided the oxidation potential ($E_{D/D+}$) lies sufficiently negative of the valence band (E_{VB}) energy level. The presence of surface defect sites creates low energy traps (E_{ST}), which in turn compete with hydrogenase for ET (k_{ST}). As observed for hybrids with high ratios of surface bound hydrogenases, k_{BET} can also contribute to lower yields of H_2 [42].

efficiencies (η_{H2}, Eq. (4)) of hydrogenase-NP complexes [41] since the recombination of electrons by surface–traps (k_{ST}) directly competes not only with k_{RR} but also with k_{ET} to the enzymes adsorbed to the NP surface.

$$\eta_{PL} = \frac{k_{RR}}{k_{RR} + k_{ST} + k_{ET}} \quad (3)$$

$$\eta_{H2} = \frac{k_{ET}}{k_{RR} + k_{ST} + k_{ET}} \quad (4)$$

Through these combined effects, the interface as defined by the ligand environment contributes to the overall energetic landscape of photocatalytic hybrid systems and helps to determine the allocation of photoexcited electrons among the various relaxation pathways. Directing ET and energy flow toward catalysis can be readily tuned in enzyme-NP hybrids by matching material compositions and geometries with appropriate ligand structures. Whereas photobiology shows unique flexibility for producing a wide-range of biofuels from sunlight, the reengineering of the basic structures that function in solar capture and energy transduction remains a considerable challenge [5].

4.2. Molecular self-assembly

The initial step for direct ET between an enzyme and a material involves formation of a molecular complex through self-assembly. This process can be designed to mimic the formation of biological protein–protein complexes that are mediated by complementary interactions of surface localized hydrophobic, polar and charged functional groups. The solvent-facing head-group of ligands has included carboxylic acid, amine, hydroxyl or hydrophobic functionalities, which can be adsorbed or cross-linked to NPs or electrodes as a mixture to provide a mosaic surface of functional groups [96,101,102]. Protein–protein ET complexes involve interfaces that are composed of polar, hydrophobic and non-polar amino acids. These participate in non-covalent contacts (e.g., charge-charge, VDW and H-bonding) and organization of the solvent and dielectric environment, all of which contribute to the overall binding strength of the interaction complex. Likewise, these interactions can be controlled in hydrogenase-NP hybrids by selection of the ligand head-groups (Fig. 3) as a means to adjust interfacial properties that affect ET.

Another important aspect to stabilizing the hybrid complex includes the interaction of the capping ligand with the semiconductor surface. In some cases the binding is photolabile, and under illumination desorption of ligands can result in the dissociation of complexes and loss of photocatalytic function. To address photolability of ligand binding, functional groups that provide chemical handles for cross-linking reactions can be added. For example diazonium terminated ligands (Fig. 3, blue panel) have been electrochemically deposited onto Au and carbon-based NPs [36,96,103,104]. Thiol-mediated binding of bidentate ligands including lipoic acid and chalcogenidometalates (e.g., thiostannates; Fig. 3, green panel) to CdSe and CdS NPs [94,95] in some cases have shown higher stability compared to mono-dentate alkane thiols. Various NPs that have predominantly aromatic surfaces, for example, single and multi-walled carbon nanotubes, have been functionalized by non-covalent attachment of aromatic ligands such as pyrene and pyrelene (Fig. 3, blue panel). These show high binding stability due to strong π–π stacking interactions, and solvent exposed head-groups can be functionalized to create a preferred type of charged surface [97,98,105].

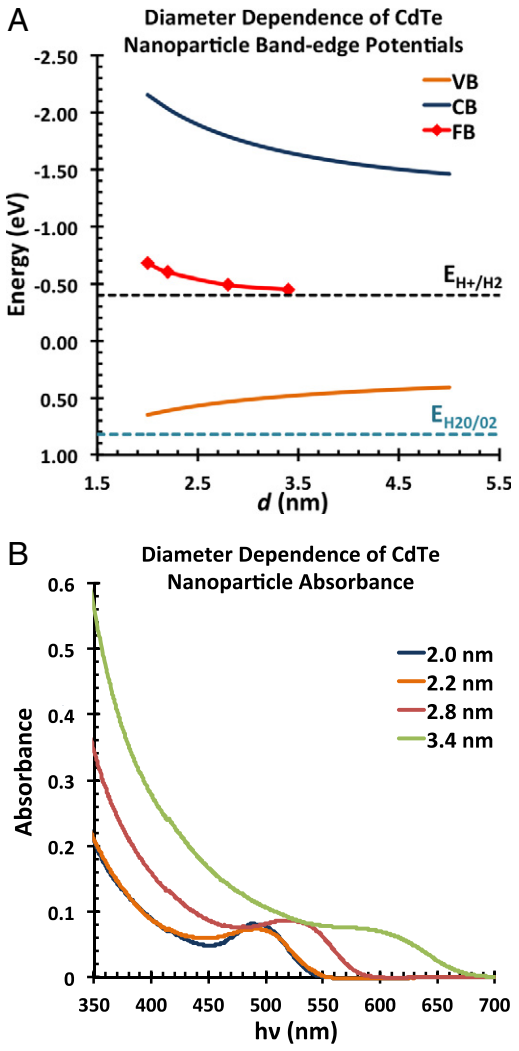

Fig. 5. Diameter dependence of the band potentials and UV-Vis absorbance spectrum of nanocrystalline CdTe. (A) Top panel. Plot of band-potential (Energy) versus CdTe NP diameter (d). The valence band (VB, orange trace) and conduction band (CB, blue trace) potentials were calculated based on fits to the equations $E_{VB} = -4.74 - 0.80d^{-0.97}$ and $E_{CB} = -3.29 + 4.19d^{-1.21}$ for VB and CB energies, respectively [91]. The calculated values are relative to vacuum, and were adjusted to the NHE scale by subtracting from −4.5 eV (value of NHE at pH = 0 relative to vacuum). The flat-band potentials (FB, red trace) are measured values for different MPA capped CdTe particles in a diameter range of 2.0–3.4 Å [79] to show the extent that optical and redox surface state energy levels can differ for CdTe. The formal potential of the H^+/H_2 (black dashed line) and H_2O/O_2 (cyan dashed line) redox couples at pH 7, 1 atm H_2 and O_2 are shown for reference. (B) Bottom panel. Plot of UV-Vis absorbance versus CdTe NP diameter (d). Plot of the inverse relationship of photon absorbance to diameter for CdTe NPs. The measured spectral response for MPA capped CdTe particles shows that both the onset and peak absorbance values shift toward the UV and increasing photon energies as the NP diameter decreases from 3.4 (green trace) to 2.0 (blue trace) nm [79].

4.3. Rate and directional control of electron-transfer in nanoparticles

The donor–acceptor distances in enzyme-NP hybrids typically exceed direct VDW contacts, and in this case k_{ET} is strongly influenced by wavefunction overlap (mixing) defined as $|H_{AB}|$ in Eq. (1). As shown in Eq. (5), $|H_{AB}|$ is attenuated by donor–acceptor distance, d, and the term β, both of which can be changed by selection of ligand properties [59].

$$|H_{AB}| = H_0 e^{-\beta d} \quad (5)$$

The differential contributions of d and β on $|H_{AB}|$ and subsequent effects on intermolecular ET have been investigated to determine the extent to which the linear and angular components of ligand orbital configurations control rates [93]. Moreover, differences in these parameters have been used to tune the bias of forward (k_{ET}) versus reverse (k_{BET}) ET in molecular systems [106]. For example, it has been suggested that the overall performance in terms of the quantum yield (QY) of converting light absorption to photocatalytic production is strongly influenced by the interplay of these effects [42]. In a series of diporphyrin linked dyads, it was shown that the degree of π-orbital symmetry determined by the angle of conjugated biphenyls (Fig. 3, gray panel) can explain an angular dependence of k_{ET} that is minimal at 45°, and nearly equally optimal at 0° or 90° [93,106]. It is difficult to envision whether or not localized steric effects can be used to control ET bias in large molecular complexes that involve many surface contacts [107]. However, this approach may provide a means to control bias through screening of ligand libraries for an increase in k_{ET}/k_{BET} using ultrafast optical techniques that probe NP carrier lifetimes in hybrid systems [49,108,109]. In addition to these observations, the operating potential of a photocatalysts has been shown to shift with an increase in d, suggesting that ligand length control of ET kinetics can be coupled to the thermodynamic control of surface catalysis [110].

5. Examples of [FeFe]-hydrogenase nanoparticle hybrids

Several reports have demonstrated the successful integration of hydrogenases with semiconducting materials [25,43] and conducting electrodes [24,27,29,41,42] and some examples are shown in Fig. 1. One of the first examples of light-driven H_2 production by a hydrogenase-semiconducting material complex was in the 1980s with [FeFe]-hydrogenase and TiO_2 [38], and more recently with dye sensitized NP-TiO_2 and [NiFeSe]-hydrogenases [44,45]. In these cases the molecular orientations were not specifically designed and optimized for ET. A design for electrostatic control of complex formation was achieved by adsorption of *Clostridial* [FeFe]-hydrogenase CaI on MPA capped NP-CdTe [41]. The ligand on CdTe binds via thiol interactions with the CdTe surface, leaving the carboxyl group exposed to solvent. As discussed above, many [FeFe]-hydrogenases, including CaI, possess positively charged regions to mediate formation of an ET complex with acidic electron carrier molecules such as ferredoxin [69,76,78,82]. Due to the high surface charge density on the NP, molecular complexes possess strong binding kinetics suggesting formation of a meta-stable complex [41,42].

Once adsorbed, the light-conversion efficiencies in [FeFe]-hydrogenase-NP hybrids show a strong dependence on the molecular compositions of the complexes [41,42]. As the hydrogenase and NPs self-assemble in solution, the resulting complexes form a distribution composed of differing stoichiometric ratios, which for hydrogenase-CdS nanorods were modeled as a Poisson distribution [42]. Photocatalysis by these and other hybrids, like in biological photosystems, occurs through the sequential process of single photoexcitation events where the macroscopic ET rate is directly proportional to incident photon flux. When molecular ratios created a high population of multiple hydrogenases per-NP, the photocatalytic conversion efficiencies were lower, presumably due to singly reduced enzymes participating in BET to the NP [42]. Thus, over a range of catalyst-NP ratios the conversion efficiencies showed dramatic differences presumably due to changes in electron allocation causing competition of photocatalysis with non-productive processes [41,42].

Hydrogenases have also been immobilized on conducting electrodes in dye-sensitized photoelectrochemical cells and biofuel cells [29,30]. In this design the charge balance is maintained by regenerating the ground state of the photoanode with an electrolyte or reforming reaction [26,111]. The conductive electrode can be composed of metal (e.g., TiO_2 or gold) or carbon (e.g. glassy carbon, pyrolytic graphite edge, carbon felt or carbon cloth) [31,34–37] based materials. Nanostructured electrodes have also been used, for example single- or multi-walled carbon nanotubes (SWNT and MWNT, respectively) or TiO_2 nanorods [27,112] on conductive supports. [FeFe]-hydrogenases and SWNTs have been shown to self-assemble into charge-transfer complexes observed by alterations in SWNT photoluminescence and Raman spectra [46]. These demonstrate

that efficient electron exchange is possible with the small intrinsic bias, between the SWNTs and hydrogenase. Thus, these can be used as highly efficient conductors for coupling redox catalysts to electrodes in solar devices.

6. Future prospects

As discussed in this review, the ligands used to passivate and functionalize NP surfaces also contribute to the control of energy flow in enzyme-NP photocatalytic hybrid systems. This control is exerted through the effects on NP geometry and energetics, molecular assembly, as well as physical parameters that mediate ET. Determining the optimal ligand properties for a particular application requires considering all of these effects and presents a significant challenge toward optimizing overall photocatalytic rates in enzyme-NP hybrids. The fact that NP charge-transfer systems have been shown to possess comparatively small reorganization energy, λ, values [113,114] versus those estimated and measured for biological ET complexes, is another facet to consider in directing energy flow toward productive reaction pathways in hybrids. In this respect, the ΔG dependence of k_{ET} for the reduction reaction can be tuned to match the formal exchange potential, and possibly constrain k_{BET} to the Marcus inverted regime (e.g., Eq. (1) where $-\Delta G^{\circ} > \lambda$) as observed for biological light conversion [7,58]. In a system based on a single light absorber, adjusting band-edges in this manner would enable more of the NP charge-separation energy to be allocated to the oxidation reaction. Water oxidation is likely to require more overpotential in order to drive slower hole-transfer (HT) reactions and achieve the desired photocatalytic rates and efficiencies. However, any advantage of a k_{ET} that is orders of magnitude faster than multi-electron oxidation catalysis will be lost if unstable reaction intermediates lead to high rates of k_{BET}.

On the other hand, assembly of enzyme-NP hybrids creates stable and more robust complexes compared to functionally equivalent biological complexes. By design must be dynamic to allow for turnover of light-driven ET that includes the interactions of electron carriers with multiple partners. Stability functionally creates a direct solar-driven ET process with photocatalytic rates that are not diffusion-limited. Moreover, for the [FeFe]-hydrogenases (and [NiFe]-hydrogenases) the intramolecular ET rates calculated from structural and thermodynamic properties are predicted to be in the range of 10^7–10^{10} s^{-1} (Section 3, and in [60]), and k_{CAT} values of immobilized enzymes measured at $\geq 10^4$ s^{-1} [86,116]. Hydrogenase-NP hybrids [41–43,45] have shown quantum efficiencies with CdTe and CdS NPs between 9 and 20% (monochromatic light) and a linear dependence on light intensity up to, and beyond, values that limit photosynthetic conversion in natural systems. Thus, through careful design of ET interfaces and tuning of NP energetics, the limiting rates of the enzymatic reactions can be explored under high photon flux, which may reveal k_{CAT} values that are faster than have been previously measured in solution [86,96,115] and a means to harness the full catalytic power of biological enzymes for H_2 production.

Acknowledgements

I would like to thank Dr. Katherine A. Brown (NREL), Prof. Gordana Dukovic (CU-Boulder), Dr. Maria L. Ghirardi (NREL), Dr. David W. Mulder (NREL), Michael W. Ratzloff (NREL) and Dr. Qing Song (IBM) for insights and helpful discussions in preparation of this manuscript, and to Drs. Brown and Song for the use of preliminary data shown in Fig. 5. I am grateful for funding support from the U.S. Department of Energy, Division of Chemical Sciences, Geosciences, and Biosciences, Office of Basic Energy Sciences; and for support by the U.S. Department of Energy under Contract No. DE-AC36-08-GO28308 with the National Renewable Energy Laboratory.

References

[1] D.I. Arnon, M. Losada, M. Nozaki, K. Tagawa, Photoproduction of hydrogen, photofixation of nitrogen and a unified concept of photosynthesis, Nature 190 (1961) 601–606.
[2] S. Eberhard, G. Finazzi, F.-A. Wollman, The dynamics of photosynthesis, Annu. Rev. Genet. 42 (2008) 463–515.
[3] M.L. Ghirardi, M.C. Posewitz, P.-C. Maness, A. Dubini, J. Yu, M. Seibert, Hydrogenases and hydrogen photoproduction in oxygenic photosynthetic organisms, Annu. Rev. Plant Biol. 58 (2007) 71–91.
[4] D. Beratan, S. Skourtis, I. Balabin, A. Balaeff, S. Keinan, R. Venkatramani, D. Xiao, Steering electrons on moving pathways, Acc. Chem. Res. 42 (2009) 1669–1678.
[5] R.E. Blankenship, D.M. Tiede, J. Barber, G.W. Brudvig, G. Fleming, M. Ghirardi, M.R. Gunner, W. Junge, D.M. Kramer, A. Melis, T.A. Moore, C.C. Moser, D.G. Nocera, A.J. Nozik, D.R. Ort, W.W. Parson, R.C. Prince, R.T. Sayre, Comparing photosynthetic and photovoltaic efficiencies and recognizing the potential for improvement, Science 332 (2011) 805–809.
[6] D. Gust, T.A. Moore, A.L. Moore, Solar fuels via artificial photosynthesis, Acc. Chem. Res. 42 (2009) 1890–1898.
[7] C.C. Moser, P.L. Dutton, Engineering protein-structure for electron-transfer function in photosynthetic reaction centers, Biochim. Biophys. Acta 1101 (1992) 171–176.
[8] L. Amirav, A.P. Alivisatos, Photocatalytic hydrogen production with tunable nanorod heterostructures, J. Phys. Chem. Lett. 1 (2010) 1051–1054.
[9] T. O'Connor, M.S. Panov, A. Mereshchenko, A.N. Tarnovsky, R. Lorek, D. Perera, G. Diederich, S. Lambright, P. Moroz, M. Zamkov, The effect of the charge-separating interface on exciton dynamics in photocatalytic colloidal heteronanocrystals, ACS Nano 6 (2012) 8156–8165.
[10] G. Dukovic, M.G. Merkle, J.H. Nelson, S.M. Hughes, A.P. Alivisatos, Photodeposition of Pt on colloidal CdS and CdSe/CdS semiconductor nanostructures, Adv. Mater. 20 (2008) 4306–4311.
[11] X.B. Chen, S.H. Shen, L.J. Guo, S.S. Mao, Semiconductor-based photocatalytic hydrogen generation, Chem. Rev. 110 (2010) 6503–6570.
[12] J.A. Cracknell, K.A. Vincent, F.A. Armstrong, Enzymes as working or inspirational electrocatalysts for fuel cells and electrolysis, Chem. Rev. 108 (2008) 2439–2461.
[13] D. Gust, T.A. Moore, A.L. Moore, Realizing artificial photosynthesis, Faraday Discuss. 155 (2012) 9–26.
[14] P.V. Kamat, Meeting the clean energy demand: nanostructure architectures for solar energy conversion, J. Phys. Chem. C 111 (2007) 2834–2860.
[15] W. Lubitz, E.J. Reijerse, J. Messinger, Solar water-splitting into H_2 and O_2: design principles of photosystem II and hydrogenases, Energy Environ. Sci. 1 (2008) 15–31.
[16] R.M. Navarro, M.C. Alvarez-Galvan, J.A. Villoria de la Mano, S.M. Al-Zahrani, J.L.G. Fierro, A framework for visible-light water splitting, Energy Environ. Sci. 3 (2010) 1865–1882.
[17] D.G. Nocera, The artificial leaf, Acc. Chem. Res. 45 (2012) 767–776.
[18] M.G. Walter, E.L. Warren, J.R. McKone, S.W. Boettcher, Q. Mi, E.A. Santori, N.S. Lewis, Solar water splitting cells, Chem. Rev. 110 (2010) 6446–6473.
[19] S.I. Allakhverdiev, V.D. Kreslavski, V. Thavasi, S.K. Zharmukhamedov, V.V. Klimov, T. Nagata, H. Nishihara, S. Ramakrishna, Hydrogen photoproduction by use of photosynthetic organisms and biomimetic systems, Photochem. Photobiol. Sci. 8 (2009) 148–156.
[20] E. Reisner, Solar hydrogen evolution with hydrogenases: from natural to hybrid systems, Eur. J. Inorg. Chem. (2011) 1005–1016.
[21] P.D. Tran, J. Barber, Proton reduction to hydrogen in biological and chemical systems, Phys. Chem. Chem. Phys. 14 (2012) 13772–13784.
[22] P.D. Tran, L.H. Wong, J. Barber, J.S.C. Loo, Recent advances in hybrid photocatalysts for solar fuel production, Energy Environ. Sci. 5 (2012) 5902–5918.
[23] M.B. Wilker, K.J. Schnitzenbaumer, G. Dukovic, Recent progress in photocatalysis mediated by colloidal II–VI nanocrystals, Isr. J. Chem. 52 (2012) 1002–1015.
[24] T.W. Woolerton, S. Sheard, Y.S. Chaudhary, F.A. Armstrong, Enzymes and bio-inspired electrocatalysts in solar fuel devices, Energy Environ. Sci. 5 (2012) 7470–7490.
[25] O.A. Zadvornyy, J.E. Lucon, R. Gerlach, N.A. Zorin, T. Douglas, T.E. Elgren, J.W. Peters, Photo-induced H_2 production by NiFe-hydrogenase from *T. roseopersicina* covalently linked to a Ru(II) photosensitizer, J. Inorg. Biochem. 106 (2012) 151–155.
[26] M. Hambourger, G. Kodis, M.D. Vaughn, G.F. Moore, D. Gust, A.L. Moore, T.A. Moore, Solar energy conversion in a photoelectrochemical biofuel cell, Dalton Trans. 45 (2009) 9979–9989.
[27] M.A. Alonso-Lomillo, O. Rudiger, A. Maroto-Valiente, M. Velez, I. Rodriguez-Ramos, F.J. Munoz, V.M. Fernandez, A.L. De Lacey, Hydrogenase-coated carbon nanotubes for efficient H_2 oxidation, Nano Lett. 7 (2007) 1603–1608.
[28] C. Baffert, K. Sybirna, P. Ezanno, T. Lautier, V. Hajj, I. Meynial-Salles, P. Soucaille, H. Bottin, C. Leger, Covalent attachment of FeFe hydrogenases to carbon electrodes for direct electron transfer, Anal. Chem. 84 (2012) 7999–8005.
[29] M. Hambourger, M. Gervaldo, D. Svedruzic, P.W. King, D. Gust, M. Ghirardi, A.L. Moore, T.A. Moore, [FeFe]-Hydrogenase catalyzed H_2 production in a photoelectrochemical biofuel cell, J. Am. Chem. Soc. 130 (2008) 2015–2022.
[30] S. Krishnan, F.A. Armstrong, Order-of-magnitude enhancement of an enzymatic hydrogen-air fuel cell based on pyrenyl carbon nanostructures, Chem. Sci. 3 (2012) 1015–1023.
[31] E. Lojou, X. Luo, M. Brugna, N. Candoni, S. Dementin, M.T. Giudici-Orticoni, Biocatalysts for fuel cells: efficient hydrogenase orientation for H_2 oxidation at electrodes modified with carbon nanotubes, J. Biol. Inorg. Chem. 13 (2008) 1157–1167.
[32] D. Svedruzic, J.L. Blackburn, R.C. Tenent, J.-D.R. Rocha, T.B. Vinzant, M.J. Heben, P.W. King, High-performance hydrogen production and oxidation electrodes with hydrogenase supported on metallic single-wall carbon nanotube networks, J. Am. Chem. Soc. 133 (2011) 4299–4306.

[33] S. Bae, E. Shim, J. Yoon, H. Joo, Photoanodic and cathodic role of anodized tubular titania in light-sensitized enzymatic hydrogen production, J. Power. Sources 185 (2008) 439–444.
[34] H. Joo, S. Bae, C. Kim, S. Kim, J. Yoon, Hydrogen evolution in enzymatic photoelectrochemical cell using modified seawater electrolytes produced by membrane desalination process, Sol. Energy Mater. Sol. Cells 93 (2009) 1555–1561.
[35] S. Morra, F. Valetti, S.J. Sadeghi, P.W. King, T. Meyer, G. Gilardi, Direct electrochemistry of an FeFe-hydrogenase on a TiO_2 electrode, Chem. Commun. 47 (2011) 10566–10568.
[36] C. Gutierrez-Sanchez, D. Olea, M. Marques, V.M. Fernandez, I.A.C. Pereira, M. Velez, A.L. De Lacey, Oriented immobilization of a membrane-bound hydrogenase onto an electrode for direct electron transfer, Langmuir 27 (2011) 6449–6457.
[37] H. Krassen, S.T. Stripp, N. Bohm, A. Berkessel, T. Happe, K. Ataka, J. Heberle, Tailor-made modification of a gold surface for the chemical binding of a high-activity FeFe hydrogenase, Eur. J. Inorg. Chem. (2011) 1138–1146.
[38] P. Cuendet, K. Rao, M. Grätzel, D. Hall, Light induced H_2 evolution in a hydrogenase-TiO_2 particle system by direct electron transfer or via rhodium complexes, Biochimie 68 (1986) 217–221.
[39] A. Selvaggi, C. Tosi, U. Barberini, E. Franchi, F. Rodriguez, P. Pedroni, *In vitro* hydrogen photoproduction using *Pyrococcus furiosus* sulfhydrogenase and TiO2, J. Photochem. Photobiol. A Chem. 125 (1999) 107–112.
[40] I.A. Shumilin, V.V. Nikandrov, V.O. Popov, A.A. Krasnovsky, Photogeneration of NADH under coupled action of CdS semiconductor and hydrogenase from *Alcaligenes eutrophus* without exogenous mediators, FEBS Lett. 306 (1992) 125–128.
[41] K.A. Brown, S. Dayal, X. Ai, G. Rumbles, P.W. King, Controlled assembly of hydrogenase-CdTe nanocrystal hybrids for solar hydrogen production, J. Am. Chem. Soc. 132 (2010) 9672–9680.
[42] K.A. Brown, M.B. Wilker, M. Boehm, G. Dukovic, P.W. King, Characterization of photochemical processes for H_2 production by CdS nanorod-[FeFe] hydrogenase complexes, J. Am. Chem. Soc. 134 (2012) 5627–5636.
[43] B.L. Greene, C.A. Joseph, M.J. Maroney, R.B. Dyer, Direct evidence of active-site reduction and photodriven catalysis in sensitized hydrogenase assemblies, J. Am. Chem. Soc. 134 (2012) 11108–11111.
[44] E. Reisner, J.C. Fontecilla-Camps, F.A. Armstrong, Catalytic electrochemistry of a [NiFeSe]-hydrogenase on TiO_2 and demonstration of its suitability for visible-light driven H_2 production, Chem. Commun. 5 (2009) 550–552.
[45] E. Reisner, D.J. Powell, C. Cavazza, J.C. Fontecilla-Camps, F.A. Armstrong, Visible light-driven H_2 production by hydrogenases attached to dye-sensitized TiO_2 nanoparticles, J. Am. Chem. Soc. 131 (2009) 18457–18466.
[46] J.L. Blackburn, D. Svedruzic, T.J. McDonald, Y.-H. Kim, P.W. King, M.J. Heben, Raman spectroscopy of charge transfer interactions between single wall carbon nanotubes and [FeFe] hydrogenase, Dalton Trans. 40 (2008) 5454–5461.
[47] T.J. McDonald, D. Svedruzic, Y.-H. Kim, J.L. Blackburn, S.B. Zhang, P.W. King, M.J. Heben, Wiring-up hydrogenase with single-walled carbon nanotubes, Nano Lett. 7 (2008) 3528–3534.
[48] J.R. Bolton, S.J. Strickler, J.S. Connolly, Limiting and realizable efficiencies of solar photolysis of water, Nature 316 (1985) 495–500.
[49] A. Nozik, Multiple exciton generation in semiconductor quantum dots, Chem. Phys. Lett. 457 (2008) 3–11.
[50] O.E. Semonin, J.M. Luther, S. Choi, H.-Y. Chen, J. Gao, A.J. Nozik, M.C. Beard, Peak external photocurrent quantum efficiency exceeding 100% via MEG in a quantum dot solar cell, Science 334 (2011) 1530–1533.
[51] C.E. Lubner, A.M. Applegate, P. Knorzer, A. Ganago, D.A. Bryant, T. Happe, J.H. Golbeck, Solar hydrogen-producing bionanodevice outperforms natural photosynthesis, Proc. Natl. Acad. Sci. U. S. A. 108 (2011) 20988–20991.
[52] L.M. Utschig, S.C. Silver, K.L. Mulfort, D.M. Tiede, Nature-driven photochemistry for catalytic solar hydrogen production: a photosystem I transition metal catalyst hybrid, J. Am. Chem. Soc. 133 (2011) 16334–16337.
[53] M. Ihara, H. Nakamoto, T. Kamachi, I. Okura, M. Maeda, Photoinduced hydrogen production by direct electron transfer from photosystem I cross-linked with cytochrome c(3) to NiFe-hydrogenase, Photochem. Photobiol. 82 (2006) 1677–1685.
[54] M. Ihara, H. Nishihara, K.S. Yoon, O. Lenz, B. Friedrich, H. Nakamoto, K. Kojima, D. Honma, T. Kamachi, I. Okura, Light-driven hydrogen production by a hybrid complex of a NiFe-hydrogenase and the cyanobacterial photosystem I, Photochem. Photobiol. 82 (2006) 676–682.
[55] H. Krassen, A. Schwarze, B. Friedrich, K. Ataka, O. Lenz, J. Heberle, Photosynthetic hydrogen production by a hybrid complex of photosystem I and NiFe-hydrogenase, ACS Nano 3 (2009) 4055–4061.
[56] R.A. Marcus, N. Sutin, Electron transfers in chemistry and biology, Biochim. Biophys. Acta 811 (1985) 265–322.
[57] D. Gust, T.A. Moore, A.L. Moore, Mimicking photosynthetic solar energy transduction, Acc. Chem. Res. 34 (2000) 40–48.
[58] A.W. Rutherford, A. Osyczka, F. Rappaport, Back-reactions, short-circuits, leaks and other energy wasteful reactions in biological electron transfer: redox tuning to survive life in O_2, FEBS Lett. 586 (2012) 603–616.
[59] H.B. Gray, J.R. Winkler, Long-range electron transfer, Proc. Natl. Acad. Sci. U. S. A. 102 (2005) 3534–3539.
[60] C.C. Page, C.C. Moser, X. Chen, P.L. Dutton, Natural engineering principles of electron tunnelling in biological oxidation-reduction, Nature 402 (1999) 47–52.
[61] S.S. Skourtis, D.H. Waldeck, D.N. Beratan, Fluctuations in biological and bioinspired electron-transfer reactions, Annu. Rev. Phys. Chem. 61 (2010) 461–485.
[62] G. McLendon, R. Hake, Interprotein electron transfer, Chem. Rev. 92 (1992) 481–490.
[63] M. Winkler, S. Kuhlgert, M. Hippler, T. Happe, Characterization of the key step for light-driven hydrogen evolution in green algae, J. Biol. Chem. 284 (2009) 36620–36627.
[64] K. Brettel, Electron transfer and arrangement of the redox cofactors in photosystem I, Biochim. Biophys. Acta 1318 (1997) 322–373.
[65] J.H. Golbeck, Structure and function of photosystem I, Annu. Rev. Plant Physiol. Plant Mol. Biol. 43 (1992) 293–324.
[66] D.C. Rees, Electrostatic influence on energetics of electron transfer reactions, Proc. Natl. Acad. Sci. U. S. A. 82 (1985) 3082–3085.
[67] L.L. Conte, C. Chothia, J. Janin, The atomic structure of protein–protein recognition sites, J. Mol. Biol. 285 (1999) 2177–2198.
[68] M.P. Fitzgerald, L.J. Rogers, K.K. Rao, D.O. Hall, Efficiency of ferredoxins and flavodoxins as mediators in systems for hydrogen evolution, Biochem. J. 192 (1980) 665–672.
[69] J.M. Moulis, V. Davasse, Probing the role of electrostatic forces in the interaction of *Clostridium pasteurianum* ferredoxin with its redox partners, Biochemistry 34 (1995) 16781–16788.
[70] K. Tagawa, D.I. Arnon, Ferredoxins as electron carriers in photosynthesis and in the biological production and consumption of hydrogen gas, Nature 195 (1962) 537–543.
[71] J. Meyer, [FeFe] hydrogenases and their evolution: a genomic perspective, Cell. Mol. Life Sci. 64 (2007) 1063–1084.
[72] P.M. Vignais, B. Billoud, Occurrence, classification, and biological function of hydrogenases: an overview, Chem. Rev. 107 (2007) 4206–4272.
[73] D.W. Mulder, E.M. Shepard, J.E. Meuser, N. Joshi, P.W. King, M.C. Posewitz, J.B. Broderick, J.W. Peters, Insights into [FeFe]-hydrogenase structure, mechanism, and maturation, Structure 19 (2011) 1038–1052.
[74] H.A. Heering, G.W. Canters, Activating redox enzymes through immobilisation and wiring, in: J.J. Davis (Ed.), Engineering the Bioelectronic Interface, Royal Society of Chemistry, Cambridge, 2009, pp. 119–152.
[75] I. Yacoby, S. Pochekailov, H. Toporik, M.L. Ghirardi, P.W. King, S. Zhang, Photosynthetic electron partitioning between [FeFe]-hydrogenase and ferredoxin: $NADP^+$-oxidoreductase (FNR) enzymes *in vitro*, Proc. Natl. Acad. Sci. U. S. A. 108 (2011) 9396–9401.
[76] C.H. Chang, P.W. King, M.L. Ghirardi, K. Kim, Atomic resolution modeling of the ferredoxin:[FeFe] hydrogenase complex from *Chlamydomonas reinhardtii*, Biophys. J. 93 (2007) 3034–3045.
[77] H. Long, C.H. Chang, P.W. King, M.L. Ghirardi, K. Kim, Brownian dynamics and molecular dynamics study of the association between hydrogenase and ferredoxin from *Chlamydomonas reinhardtii*, Biophys. J. 95 (2008) 3753–3766.
[78] H. Long, P.W. King, M.L. Ghirardi, K. Kim, Hydrogenase/ferredoxin charge-transfer complexes: effect of hydrogenase mutations on the complex association, J. Phys. Chem. A 113 (2009) 4060–4067.
[79] K.A. Brown, Q. Song, Unpublised results (2013).
[80] A.S. Pandey, T.V. Harris, L.J. Giles, J.W. Peters, R.K. Szilagyi, Dithiomethylether as a ligand in the hydrogenase H-cluster, J. Am. Chem. Soc. 130 (2008) 4533–4540.
[81] J.W. Peters, W.N. Lanzilotta, B.J. Lemon, L.C. Seefeldt, X-ray crystal structure of the Fe-only hydrogenase (CpI) from *Clostridium pasteurianum* to 1.8 angstrom resolution, Science 282 (1998) 1853–1858.
[82] J.W. Peters, Structure and mechanism of iron-only hydrogenases, Curr. Opin. Struct. Biol. 9 (1999) 670–676.
[83] M.W. Adams, E. Eccleston, J.B. Howard, Iron-sulfur clusters of hydrogenase I and hydrogenase II of *Clostridium pasteurianum*, Proc. Natl. Acad. Sci. U. S. A. 86 (1989) 4932–4936.
[84] F.A. Armstrong, J. Hirst, Reversibility and efficiency in electrocatalytic energy conversion and lessons from enzymes, Proc. Natl. Acad. Sci. U. S. A. 108 (2011) 14049–14054.
[85] F.A. Armstrong, G.S. Wilson, Recent developments in faradaic bioelectrochemistry, Electrochim. Acta 45 (2000) 2623–2645.
[86] C. Madden, M.D. Vaughn, I. Diez-Perez, K.A. Brown, P.W. King, D. Gust, A.L. Moore, T.A. Moore, Catalytic turnover of FeFe-hydrogenase based on single-molecule imaging, J. Am. Chem. Soc. 134 (2012) 1577–1582.
[87] X. Ai, Q. Xu, M. Jones, Q. Song, S.Y. Ding, R.J. Ellingson, M. Himmel, G. Rumbles, Photophysics of (CdSe) ZnS colloidal quantum dots in an aqueous environment stabilized with amino acids and genetically-modified proteins, Photochem. Photobiol. Sci. 6 (2007) 1027–1033.
[88] M. Amelia, S. Impellizzeri, S. Monaco, I. Yildiz, S. Silvi, F.M. Raymo, A. Credi, Structural and size effects on the spectroscopic and redox properties of CdSe nanocrystals in solution: the role of defect states, ChemPhysChem 12 (2011) 2280–2288.
[89] T. Rajh, O.I. Micic, A.J. Nozik, Synthesis and characterization of surface-modified colloidal cadmium telluride quantum dots, J. Phys. Chem. 97 (1993) 11999–12003.
[90] Y.-h. Zhang, H.-s. Zhang, M. Ma, X.-f. Guo, H. Wang, The influence of ligands on the preparation and optical properties of water-soluble CdTe quantum dots, Appl. Surf. Sci. 255 (2009) 4747–4753.
[91] J. Jasieniak, M. Califano, S.E. Watkins, Size-dependent valence and conduction band-edge energies of semiconductor nanocrystals, ACS Nano 5 (2011) 5888–5902.
[92] S. Chen, L.-W. Wang, Thermodynamic oxidation and reduction potentials of photocatalytic semiconductors in aqueous solution, Chem. Mater. 24 (2012) 3659–3666.
[93] A. Helms, D. Heiler, G. McLendon, Dependence of electron transfer rates on donor–acceptor angle in bis-porphyrin adducts, J. Am. Chem. Soc. 113 (1991) 4325–4327.
[94] Z. Han, F. Qiu, R. Eisenberg, P.L. Holland, T.D. Krauss, Robust photogeneration of H2 in water using semiconductor nanocrystals and a nickel catalyst, Science 338 (2012) 1321–1324.
[95] A.A. Cordones, M. Scheele, A.P. Alivisatos, S.R. Leone, Probing the interaction of single nanocrystals with inorganic capping ligands: time-resolved fluorescence

from CdSe–CdS quantum dots capped with chalcogenidometalates, J. Am. Chem. Soc. 134 (2012) 18366–18373.
[96] C. Gutiérrez-Sánchez, M. Pita, C. Vaz-Domínguez, S. Shleev, A.L. De Lacey, Gold nanoparticles as electronic bridges for laccase-based biocathodes, J. Am. Chem. Soc. 134 (2012) 17212–17220.
[97] C. Ehli, C. Oelsner, D.M. Guldi, A. Mateo-Alonso, M. Prato, C. Schmidt, C. Backes, F. Hauke, A. Hirsch, Manipulating single-wall carbon nanotubes by chemical doping and charge transfer with perylene dyes, Nat. Chem. 1 (2009) 243–249.
[98] C. Oelsner, C. Schmidt, F. Hauke, M. Prato, A. Hirsch, D.M. Guldi, Interfacing strong electron acceptors with single wall carbon nanotubes, J. Am. Chem. Soc. 133 (2011) 4580–4586.
[99] S. Yang, D. Prendergast, J.B. Neaton, Tuning semiconductor band edge energies for solar photocatalysis via surface ligand passivation, Nano Lett. 12 (2011) 383–388.
[100] D.A.R. Barkhouse, A.G. Pattantyus-Abraham, L. Levina, E.H. Sargent, Thiols passivate recombination centers in colloidal quantum dots leading to enhanced photovoltaic device efficiency, ACS Nano 2 (2008) 2356–2362.
[101] A.M. Jackson, Y. Hu, P.J. Silva, F. Stellacci, From homoligand- to mixed-ligand-monolayer-protected metal nanoparticles: a scanning tunneling microscopy investigation, J. Am. Chem. Soc. 128 (2006) 11135–11149.
[102] T. Tsuruoka, K. Akamatsu, H. Nawafune, Synthesis, surface modification, and multilayer construction of mixed-monolayer-protected CdS nanoparticles, Langmuir 20 (2004) 11169–11174.
[103] A. Kowalczyk, M. Fau, A.M. Nowicka, Z. Stojek, Formation of intermediate layers for immobilization of biomacromolecules by self-assembling and reduction of phenyldiazonium salts. A comparative study, Electroanalysis 24 (2012) 2053–2060.
[104] M.S. Strano, C.A. Dyke, M.L. Usrey, P.W. Barone, M.J. Allen, H. Shan, C. Kittrell, R.H. Hauge, J.M. Tour, R.E. Smalley, Electronic structure control of single-walled carbon nanotube functionalization, Science 301 (2003) 1519–1522.
[105] D.M. Guldi, G.M.A. Rahman, F. Zerbetto, M. Prato, Carbon nanotubes in electron donor–acceptor nanocomposites, Acc. Chem. Res. 38 (2005) 871–878.
[106] A.C. Benniston, A. Harriman, Charge on the move: how electron-transfer dynamics depend on molecular conformation, Chem. Soc. Rev. 35 (2006) 169–179.
[107] A. Osuka, K. Maruyama, N. Mataga, T. Asahi, I. Yamazaki, N. Tamai, Geometry dependence of intramolecular photoinduced electron transfer in synthetic zinc-ferric hybrid diporphyrins, J. Am. Chem. Soc. 112 (1990) 4958–4959.
[108] R.H. Goldsmith, L.E. Sinks, R.F. Kelley, L.J. Betzen, W. Liu, E.A. Weiss, M.A. Ratner, M.R. Wasielewski, Wire-like charge transport at near constant bridge energy through fluorene oligomers, Proc. Natl. Acad. Sci. U. S. A. 102 (2005) 3540–3545.
[109] O. Wenger, How donor–bridge–acceptor energetics influence electron tunneling dynamics and their distance dependences, Acc. Chem. Res. 44 (2011) 25–35.
[110] A.A. Gambardella, S.W. Feldberg, R.W. Murray, Electron transfer dynamics of iridium oxide nanoparticles attached to electrodes by self-assembled monolayers, J. Am. Chem. Soc. 134 (2012) 5774–5777.
[111] M. Hambourger, P.A. Liddell, D. Gust, A.L. Moore, T.A. Moore, Parameters affecting the chemical work output of a hybrid photoelectrochemical biofuel cell, Photochem. Photobiol. Sci. 6 (2007) 431–437.
[112] B. Bae, B.K. Kho, T.-H. Lim, I.-H. Oh, S.-A. Hong, H.Y. Ha, Performance evaluation of passive DMFC single cells, J. Power Sources 158 (2006) 1256–1261.
[113] G.D. Scholes, M. Jones, S. Kumar, Energetics of photoinduced electron-transfer reactions decided by quantum confinement, J. Phys. Chem. C 111 (2007) 13777–13785.
[114] K. Tvrdy, P.A. Frantsuzov, P.V. Kamat, Photoinduced electron transfer from semiconductor quantum dots to metal oxide nanoparticles, Proc. Natl. Acad. Sci. U. S. A. 108 (2011) 29–34.
[115] H.R. Pershad, J.L.C. Duff, H.A. Heering, E.C. Duin, S.P.J. Albracht, F.A. Armstrong, Catalytic electron transport in chromatium vinosum [NiFe]-hydrogenase: application of voltammetry in detecting redox-active centers and establishing that hydrogen oxidation is very fast even at potentials close to the reversible H^+/H_2 value, Biochemistry 38 (1999) 8992–8999.